

Non-diffusive angular momentum transport in rotating z -pinches †

G. Rüdiger‡, M. Schultz

Leibniz-Institut für Astrophysik Potsdam, An der Sternwarte 16, D-14482 Potsdam, Germany

(Received xx; revised xx; accepted xx)

The stability of conducting Taylor-Couette flows under the presence of toroidal magnetic background fields is considered. For strong enough magnetic amplitudes such magnetohydrodynamic flows are unstable against nonaxisymmetric perturbations which may also transport angular momentum. In accordance with the often used diffusion approximation one expects the angular momentum transport vanishing for rigid rotation. In the sense of a nondiffusive Λ effect, however, even for *rigidly* rotating z -pinches an axisymmetric angular momentum flux appears which is directed outward (inward) for large (small) magnetic Mach numbers. The internal rotation in a magnetized rotating tank can thus never be uniform. Those particular rotation laws are used to estimate the value of the instability-induced eddy viscosity for which the nondiffusive Λ effect and the diffusive shear-induced transport compensate each other. The results provide the well-known Shakura & Sunyaev (1973) viscosity ansatz leading to numerical values linearly growing with the Reynolds number of rotation.

Key words: Angular momentum transport – azimuthal magnetorotational instability – rotating z -pinch – diffusion approximation

1. Introduction

A hydrodynamic Taylor-Couette flow with rotation profiles beyond the Rayleigh limit is stable against axi- and nonaxisymmetric perturbations. It is unstable, however, against axisymmetric perturbations under the presence of axial magnetic background fields (Velikhov 1959; Rüdiger & Zhang 2001; Ji *et al.* 2001)) and it is unstable against nonaxisymmetric perturbations under the presence of azimuthal fields (Taylor 1957; Ogilvie & Pringle 1996). For axial fields and given magnetic Prandtl number

$$P_m = \frac{\nu}{\eta} \quad (1.1)$$

(with molecular viscosity ν and magnetic resistivity η) there exists always a critical magnetic field amplitude with a minimal Reynolds number. These numbers are running with $1/P_m$ so that for the small magnetic Prandtl numbers of liquid metals the critical Reynolds numbers basically exceed values of 10^6 (Rüdiger & Shalybkov 2001). This very high Reynolds number is the main reason that to date the standard magnetorotational instability has not yet been realized in laboratory experiments.

For much lower critical Reynolds numbers the Couette flow becomes unstable if the magnetic background field is toroidal or has a toroidal component. Herron & Soliman (2006) demonstrated that all flows with negative shear and current-free background fields are stable against axisymmetric perturbations. There and also here the flows are assumed as unbounded in the axial direction. The existing instabilities must thus always be nonaxisymmetric. For the absolutely

† 22 July 2019

‡ Email address for correspondence: gruediger@aip.de

lowest possible magnetic field amplitude the critical Reynolds number for the onset of this so-called Azimuthal MagnetoRotational Instability (AMRI) for liquid metals such as gallium or sodium is only $O(10^3)$, hence there is a very strong reduction compared with the Reynolds numbers needed for the magnetorotational instability with axial fields. Not surprisingly, the AMRI at and slightly beyond the Rayleigh line has already been realized in the laboratory (Seilmayer *et al.* 2014).

The nonaxisymmetric AMRI also exists for flows rotating with a positive shear $d\Omega/dR$ (“super-rotation”). This is insofar of relevance as super-rotating Taylor-Couette flows are prototypes of very stable hydrodynamic flows (but see Deguchi (2017) for a nonaxisymmetric instability at high Reynolds numbers). For conducting fluids with magnetic Prandtl numbers less or larger than unity such flows can easily be destabilized with supercritical toroidal magnetic fields. The needed Reynolds numbers (of the outer cylinder) for flows with stationary inner cylinder are only $O(100)$, see Stefani & Kirillov (2015); Rüdiger *et al.* (2018).

Another instability exists for conducting fluids wherein axial electric currents produce azimuthal magnetic fields of radial profiles less steep than the vacuum profile $1/R$ where R is the radius in cylindrical coordinates. The relation

$$\frac{d}{dR}(RB_\phi^2) \leq 0 \quad (1.2)$$

is a sufficient and necessary condition for stability of a stationary ideal fluid against nonaxisymmetric perturbations (Taylor 1973). One finds instability in particular for the azimuthal field with the radial profile $B_\phi \propto R$ produced by a uniform electric current. The existence of a nonaxisymmetric instability for such a (nonrotating) z -pinch has been shown by Seilmayer *et al.* (2012) using the liquid GaInSn alloy as the conducting fluid penetrated by an axial electric current of $\simeq 3$ kAmp.

The combination of a current-free magnetic field $B_\phi \propto 1/R$ and the rotation profile $\Omega \propto 1/R^2$ of the potential flow belongs to a particular class of MHD flows defined by the condition that the magnetic Mach number Mm in the relation

$$U = Mm U_A, \quad (1.3)$$

with U the flow velocity and $U_A = B/\sqrt{\mu_0\rho}$ its Alfvén speed, is a constant value (Chandrasekhar 1956). Applied to Taylor-Couette flows the radial profiles of the flow velocity U_ϕ and B_ϕ are required as identical. All such flows are stable in the absence of diffusive effects. On the other hand, it is known that the potential flow of real fluids with $\Omega \propto 1/R^2$ can easily be destabilized by the current-free toroidal magnetic field with $B_\phi \propto 1/R$ (Rüdiger *et al.* 2007). All these MHD flows possess marginal instabilities for Reynolds numbers as a function of Hartmann numbers where these values do not depend on Pm for $Pm \rightarrow 0$. Even in the inductionless approximation $Pm = 0$ these eigenvalues remain finite. A prominent example is also the rigidly rotating z -pinch where the flow U_ϕ and the field B_ϕ are both proportionate to the cylinder radius R .

This sort of Taylor-Couette flows will be considered in the present paper to probe its qualification to transport angular momentum. In the cylinder coordinates used for Taylor-Couette flows (unbounded in z) only the radial component T_R of the total stress tensor must be considered which is formed by the $(R\phi)$ components of the difference of Reynolds stress and Maxwell stress. In the so-called diffusion approximation the T_R component has been written as

$$T_R = -\nu_T R \frac{d\Omega}{dR}, \quad (1.4)$$

with positive eddy viscosity ν_T . Such a relation has originally been formulated for hydrodynamical turbulence (Boussinesq 1897) based on the observation that in a rigidly rotating fluid

no angular momentum is transported. We shall see, however, that for the pinch-type instability the diffusion approximation (1.4) does not hold for uniform rotation. This gives a new possibility to estimate the magnetic-instability-induced turbulent viscosity for differentially rotating magnetized containers. The resulting expression can also be considered as a confirmation of the viscosity approximation introduced by Shakura & Sunyaev (1973) and Pringle (1981) to the accretion disk theory as an explanation of the angular momentum transport in thin disks.

Furthermore, some important applications of stellar physics are based on the Eq. (1.4). We know from helioseismology that the solar radiative core rotates rigidly. One needs effective viscosities of 10^4 times the molecular value to explain the decay of an initial rotation law within the lifetime of the Sun. Also the Maxwell stress theory of this decay needs an increase of the microscopic viscosity by a few orders of magnitude for the explanation of the rigid rotation (Charbonneau & MacGregor 1992; Rüdiger & Kitchatinov 1996). It remains to test whether the angular momentum transport by magnetic instabilities of fossil internal toroidal fields is strong enough to produce the quasi-uniform inner rotation of the Sun.

The lithium at the surface of cool main-sequence stars decays with a timescale of 1 Gyr. It is burned at temperatures in excess of 2.6×10^6 K, which exists about 40.000 km below the base of the solar convection zone. There must be a diffusion process down to this layer with the burning temperature. A slow transport process is needed which is only one or two orders of magnitude faster than the molecular diffusion. The molecular diffusion beneath the solar convection zone must be increased but only to about 10^3 cm²/s.

In this paper we present the linear theory of rigidly rotating z -pinches (with homogeneous axial electric current) for two sorts of boundary conditions in order to calculate the instability-induced normalized radial transport of angular momentum. The basic equations of magnetohydrodynamics (MHD) are presented in Sect. 2. The eigenfunctions of the unstable solutions and the instability-originated angular momentum transport (its “ Λ effect”) for given magnetic Prandtl number are presented in Sect. 3. The transition to differential rotation also in terms of an eddy viscosity is discussed in Sect. 4 while Sect. 5 contains a short discussion of the results.

2. The Equations

The equations of the magnetic-instability theory are the well-known MHD equations

$$\begin{aligned} \frac{\partial \mathbf{U}}{\partial t} + (\mathbf{U} \cdot \nabla) \mathbf{U} &= -\frac{1}{\rho} \nabla P + \nu \Delta \mathbf{U} + \frac{1}{\mu_0 \rho} \text{curl} \mathbf{B} \times \mathbf{B}, \\ \frac{\partial \mathbf{B}}{\partial t} &= \text{curl}(\mathbf{U} \times \mathbf{B}) + \eta \Delta \mathbf{B} \end{aligned} \quad (2.1)$$

with $\text{div} \mathbf{U} = \text{div} \mathbf{B} = 0$ for an incompressible fluid. \mathbf{U} is the velocity vector, \mathbf{B} the magnetic field vector and P the pressure. The basic state in the cylindric system with the coordinates (R, ϕ, z) is $U_R = U_z = B_R = B_z = 0$ for the poloidal components and

$$\Omega = a + \frac{b}{R^2} \quad (2.2)$$

for the rotation law with the constants $a = \Omega_{\text{in}}(\mu - r_{\text{in}}^2)/(1 - r_{\text{in}}^2)$ and $b = \Omega_{\text{in}} R_{\text{in}}^2(1 - \mu)/(1 - r_{\text{in}}^2)$. Here $r_{\text{in}} = R_{\text{in}}/R_{\text{out}}$ is the ratio of the inner cylinder radius R_{in} and the outer cylinder radius R_{out} . Ω_{in} and Ω_{out} are the angular velocities of the inner and outer cylinders, respectively. With the definition

$$\mu = \frac{\Omega_{\text{out}}}{\Omega_{\text{in}}} \quad (2.3)$$

$\mu = 1$ describes solid-body rotation with uniform Ω while $\mu < 1$ belongs to rotation laws with negative radial shear (“sub-rotation”). Super-rotation (positive shear, $d\Omega/dR > 0$) leads to $\mu > 1$.

The stationary solution for the magnetic field which is current-free in the fluid is $B_\phi = B_{\text{in}}R_{\text{in}}/R$. We define $\mu_B = B_{\text{out}}/B_{\text{in}}$, hence $\mu_B = r_{\text{in}}$. For pinch-type solutions due to homogeneous axial electric currents with $B_\phi = B_{\text{in}}R/R_{\text{in}}$ it is $\mu_B = 1/r_{\text{in}}$.

The dimensionless physical parameters of the system besides the magnetic Prandtl number are the Hartmann number Ha and the Reynolds number Re ,

$$\text{Ha} = \frac{B_{\text{in}}D}{\sqrt{\mu_0\rho\nu\eta}}, \quad \text{Re} = \frac{\Omega_{\text{in}}D^2}{\nu}. \quad (2.4)$$

The difference $D = R_{\text{out}} - R_{\text{in}}$ is the gap width between the cylinders. The Hartmann number is defined with the magnetic field at the inner wall. The ratio of the angular velocity of rotation and the Alfvén frequency of the magnetic field is the magnetic Mach number Mm which easily can be expressed by the magnetic Prandtl number, the Reynolds number and the Hartmann number, i.e.

$$\text{Mm} = \frac{\Omega_{\text{in}}}{\Omega_{\text{A},\text{in}}} = \frac{\sqrt{\text{PmRe}}}{\text{Ha}}. \quad (2.5)$$

Fast rotation compared with the magnetic field is described by $\text{Mm} > 1$ and slow rotation by $\text{Mm} < 1$. $\text{Mm} = 1$ may be called a magnetic sonic point. Many cosmical objects can be characterized by $\text{Mm} > 1$.

The variables \mathbf{U} , \mathbf{B} and P are split into mean and fluctuating components, i.e. $\mathbf{U} = \bar{\mathbf{U}} + \mathbf{u}$, $\mathbf{B} = \bar{\mathbf{B}} + \mathbf{b}$ and $P = \bar{P} + p$. The bars from the mean-field variables are immediately dropped, so that the capital letters \mathbf{U} , \mathbf{B} and P represent the background quantities. Simplifying, the nonaxisymmetric components of flow and field may be used in the following as the fluctuations while the axisymmetric components are considered as the mean quantities. Then the averaging procedure is the integration over the azimuth ϕ . By developing the fluctuations \mathbf{u} , \mathbf{b} and p into normal modes, $[\mathbf{u}, \mathbf{b}, p] = [\mathbf{u}(R), \mathbf{b}(R), p(R)]\exp(i(\omega t + kz + m\phi))$, the solutions of the linearized MHD equations are considered for axially unbounded cylinders. Here k is the axial wave number of the perturbation, m its azimuthal wave number and ω the complex frequency including growth rate as its negative imaginary part and a drift frequency ω_{dr} as its real part. A numerical code is used to solve the resulting set of linearized ordinary differential equations for the radial functions of flow, field and pressure fluctuations. The solutions are optimized with respect to the Reynolds number for given Hartmann number by varying the wave number. Only solutions for $|m| = 1$ are here discussed. For consistency only such small Hartmann numbers are considered for which only these lowest unstable modes are excited.

2.1. Boundary conditions

The hydrodynamic boundary conditions at the cylinder walls are the rigid ones, i.e. $u_R = u_\phi = u_z = 0$. The cylinders are either considered as perfectly conducting or insulating. For the conducting walls the fluctuations must fulfill $db_\phi/dR + b_\phi/R = b_R = 0$ at R_{in} and R_{out} so that ten boundary conditions exist for the set of ten differential equations. The magnetic boundary conditions for insulating walls are much more complicated, i.e.

$$b_R + \frac{ib_z}{I_m(kR)} \left(\frac{m}{kR} I_m(kR) + I_{m+1}(kR) \right) = 0 \quad (2.6)$$

for $R = R_{\text{in}}$ and

$$b_R + \frac{ib_z}{K_m(kR)} \left(\frac{m}{kR} K_m(kR) - K_{m+1}(kR) \right) = 0 \quad (2.7)$$

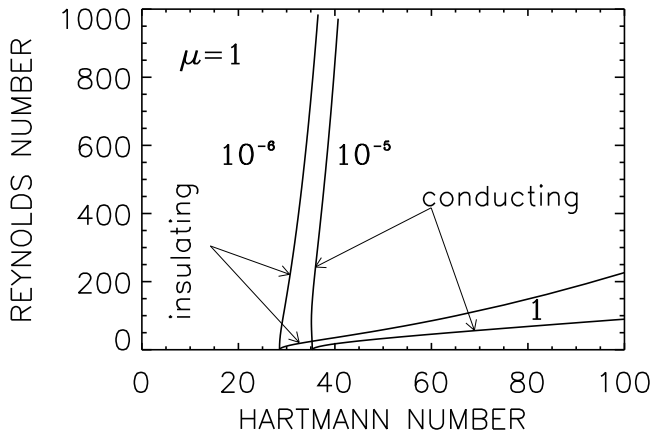


FIGURE 1. Stability map $Re_{\max} = Re_{\max}(Ha)$ for z -pinch with rigid rotation for small and large magnetic Prandtl numbers (marked). Models with parameters below the lines are unstable. Both boundary conditions: perfect-conducting as well as insulating cylinders. $\mu = 1$, $\mu_B = 2$, $r_{\text{in}} = 0.5$, $m = \pm 1$.

for $R = R_{\text{out}}$, where I_m and K_m are the modified Bessel functions of second kind. The conditions for the toroidal field are simply $kRb_\phi = mb_z$ at R_{in} and R_{out} . More details including the modified expressions for cylinders with *finite* electric conductivity have been given by Rüdiger *et al.* (2018).

For the magnetic field with $\mu_B = 1/r_{\text{in}}$ the Fig. 1 shows the lines of neutral stability (i.e. for vanishing growth rate) for the rigidly rotating flow ($\mu = 1$) for both sorts of boundary conditions. The Taylor instability for $m = \pm 1$ exists for supercritical Hartmann numbers. Absolute minima Ha_0 of the Hartmann numbers exist below which the rotation law is stable. The curve of neutral instability limits the instability by suppressing the nonaxisymmetric field mode by too fast rotation.

To demonstrate the influence of the boundary condition the Fig. 1 gives the instability lines for containers with perfect-conducting and insulating cylinders. The $Ha_0 = 28.1$ for vacuum conditions prove to be smaller than the $Ha_0 = 35.3$ for perfect-conducting conditions. With insulating cylinders the magnetized Taylor-Couette flows become more easily unstable than with conducting cylinders.

As already noted the magnetized flow of Fig. 1 constitutes a standard example of the Chandrasekhar-type flows. The relations $\Omega \propto R^{-q}$ and $B_\phi \propto R^{1-q}$ defining these flows in Taylor-Couette systems lead to the Chandrasekhar condition

$$\mu = r_{\text{in}}\mu_B, \quad (2.8)$$

hence $\mu_B = 2\mu$ for $r_{\text{in}} = 0.5$. This general condition is fulfilled for the rigidly rotating z -pinch with $\mu = 1$ and $\mu_B = 2$. The lines of marginal stability of the flow basically coincide in the (Ha/Re) plane for $Pm \rightarrow 0$. All curves for small Pm of Fig. 1 are thus identical (and invisible).

The magnetic Prandtl number of $Pm = 10^{-5}$ characterizes liquid sodium as the conducting fluid. The plotted lines of marginal instability are valid for all $Pm \leq 10^{-5}$ including $Pm = 0$. They thus can also be obtained by use of the inductionless approximation.

The z -pinch is characterized by a homogeneous electric current in axial direction which becomes unstable even without rotation if the current is strong enough. As is also demonstrated by the instability map the numerical value of Ha_0 does (slightly) depend on the boundary conditions but does not depend on the magnetic Prandtl number. On the other hand, however, the

rotational suppression of the Tayler instability strongly depends on the magnetic Prandtl number. For the very small Pm it almost disappears. The curves in Fig 1 can also be characterized by magnetic Mach numbers which are almost independent of the numerical value of the Hartmann number. Obviously the magnetic Mach number slightly exceeds unity for $Pm \simeq 1$ but it becomes smaller for smaller Pm. As it is true for all Chandrasekhar-type flows (which scale with Ha and Re for $Pm \rightarrow 0$) the magnetic Mach number decreases with decreasing \sqrt{Pm} for very small Pm which limits the astrophysical relevance of the instability for objects of small magnetic Prandtl number.

2.2. Angular momentum transport

It is known that the radial angular momentum transport by instability patterns can be described by the $(R\phi)$ component of the total stress tensor,

$$T_{ij} = \langle u_i u_j \rangle - \frac{1}{\mu_0 \rho} \langle b_i b_j \rangle + \frac{1}{2\mu_0 \rho} \langle \mathbf{b}^2 \rangle \delta_{ij}, \quad (2.9)$$

as the difference

$$T_R = \langle u_R u_\phi \rangle - \frac{1}{\mu_0 \rho} \langle b_R b_\phi \rangle \quad (2.10)$$

of the Reynolds and Maxwell stress tensors taken at the same spatial and temporal coordinates. In the diffusion approximation (1.4) this tensor component is assumed as existing only for non-uniform rotation, representing angular momentum as flowing in the direction of slower rotation (for positive ν_T). To probe the applicability of the diffusion approximation we shall compute (2.10) for magnetic instabilities. As the Tayler instability even exists for rigid rotation its angular momentum transport should vanish. We shall calculate the radial flux of the angular momentum (2.10) along the lines of neutral stability where it is allowed to use the linearized MHD equations.

3. Rotating z-pinches

The z -pinch is formed by an uniform electric current throughout the entire region $R < R_{\text{out}}$. Any resulting instability is purely current-driven, it even exists for $Re = 0$, the rotation only acts suppressing (Pitts & Tayler 1985). The curves of Fig. 1 demonstrate the stabilizing effect of rotation which is strongest for $Pm = 1$. It becomes weaker for smaller magnetic Prandtl numbers. In all cases a maximal Reynolds number Re_{max} exists for given Hartmann number above which the z -pinch is stable. The Re_{max} defining the Reynolds number of neutral stability depends on the magnetic Prandtl number, i.e. the smaller the Pm the higher the Re_{max} . Quasi-Keplerian flow of $Ha = 50$ allows instability only up to $Re_{\text{max}} \simeq 1000$ for $Pm = 1$ and $\simeq 3000$ for $Pm = 0.01$ independent of the used boundary conditions.

3.1. The eigenfunctions

The homogeneous system of differential equations for the perturbations forms an eigenvalue problem with eigensolutions for $\mathbf{u}(R)$ and $\mathbf{b}(R)$ which can be determined up to a free real multiplication factor. The sign of products of two perturbation components, therefore, remains unchanged. For the mode with $m = 1$ these functions in their dependence on R are given in Fig. 2 for $Pm = 0.1$. Note the boundary conditions $\mathbf{u} = 0$ and $b_R = 0$ (for perfect-conducting walls) as fulfilled. One also finds, as it must, for $m = -1$ the components u_R, u_ϕ, b_R and b_ϕ are conjugate-complex as also the field components $-iu_z$ and $-ib_z$ are. It means that for the transformation $m \rightarrow -m$ the components b_R transform as $b_R^R \rightarrow b_R^R$ and $b_R^I \rightarrow -b_R^I$ (the same for b_ϕ) while for $m \rightarrow -m$ it is $b_z^R \rightarrow -b_z^R$ and $b_z^I \rightarrow b_z^I$. The superscripts R stand for the real parts and I for the imaginary parts of the eigensolutions.

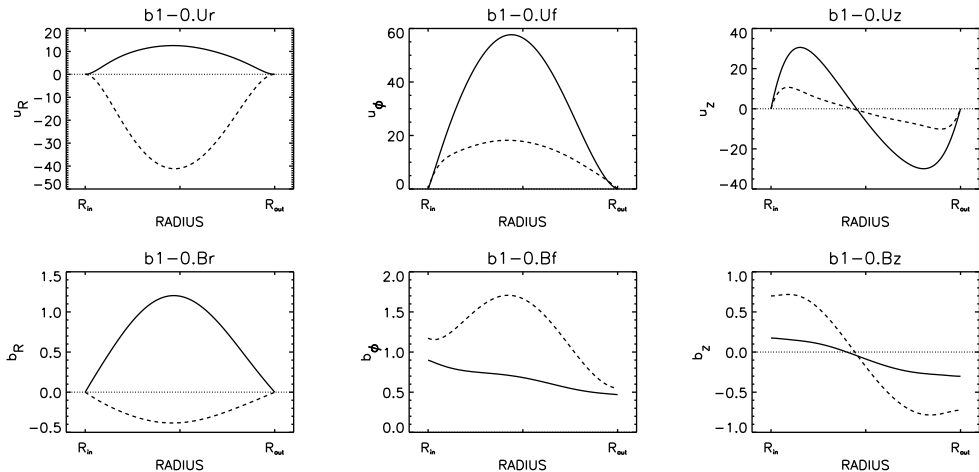


FIGURE 2. Eigenfunctions (real parts: solid lines; imaginary parts: dashed lines) of the rigidly rotating z -pinch for $\text{Ha} = 50$ and $\text{Re} = 144$ for perfect-conducting boundary conditions. $r_{\text{in}} = 0.5$. $m = 1$, $\text{Pm} = 0.1$, $\mu_B = 2$, $\mu = 1$.

The product of two scalars A and B after averaging over the ϕ coordinate is the sum of the products of the real parts and the imaginary parts, i.e. $AB = A^R B^R + A^I B^I$. There is a certain factor in front of this expression whose value, however, is unimportant as in the linear theory the vector components are only known up to a free factor. In Fig. 2 the magnetic-induced contribution $b_R b_\phi$ to the radial flux of angular momentum is positive. One expects $b_R b_\phi \simeq 0$ for rigid rotation which, however, is here not the case. As the kinetic transport $u_R u_\phi$ is (slightly) negative the total stress component T_R is negative, too.

The plotted amplitudes of the functions are completely arbitrary, they have no physical meaning. The above given sign rules for the products of radial and azimuthal components of flow and fields are not influenced by the boundary conditions. As with our normalizations the total stress results from the difference $\langle u_R u_\phi \rangle - \text{PmHa}^2 \langle b_R b_\phi \rangle$ (where the instability sets in for almost constant Ha if $\text{Pm} \rightarrow 0$) the sign of the angular momentum transport is determined by the flow perturbations for small Pm and by the magnetic fluctuations for large Pm . The torque on the cylinders obviously vanishes if by the boundary conditions $u_R = b_R = 0$. The average procedure may concern the cylinder surface formed by z and ϕ . Then it becomes $\langle u_R u_\phi \rangle \propto u_R^R u_\phi^R + u_R^I u_\phi^I$. All the terms mixed in R and I disappear after averaging over the azimuth ϕ . The same procedure holds for the magnetic terms. From the transformation rules for $m \rightarrow -m$ it is clear that the modes m and $-m$ lead to the same flux of angular momentum. The curves for T_R in Fig. 3 are thus identical for $m = 1$ and $m = -1$.

We have to normalize the expression (2.10) in order to compensate the role of the free parameter in the eigenfunctions. To this end the T_R is divided by the total energy $E = \langle \mathbf{u}^2 \rangle + \langle \mathbf{b}^2 \rangle / \mu_0 \rho$ (in our units $E = \langle \mathbf{u}^2 \rangle + \text{PmHa}^2 \langle \mathbf{b}^2 \rangle$). According to this definition the normalized $|T_R|$ should not exceed unity.

The angular momentum transport by the current-driven Tayler instability with $\mu_B = 2$ and $\mu = 1$ is given by Fig. 3 for a fixed Hartmann number; $\text{Ha} = 50$. The flow is of the Chandrasekhar-type and because of its uniform rotation angular momentum should not be transported but it does. Note the negative value for $\text{Pm} \lesssim 0.1$ which has been suggested above by inspection of Fig. 2. Generally, the transport direction depends on the magnetic Prandtl number but its absolute value $|T_R|$ becomes very small for the smallest magnetic Prandtl numbers. After Eq. (1.4) the angular

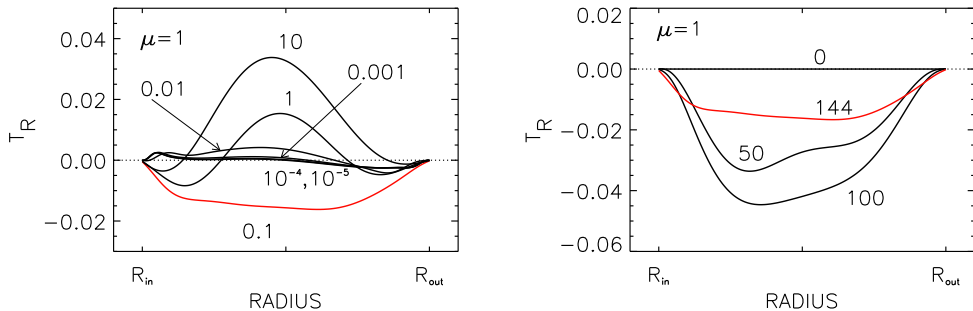


FIGURE 3. Normalized angular momentum transport $T_R(R)$ as a function of the radius R for the z -pinch with rigid rotation. Left: variation of Pm (marked) for neutral stability ($Re = Re_{\max}$), right: variation of Re (marked) for fixed $Pm = 0.1$ (vertical cut in the stability map). The curves are identical for $m \rightarrow -m$. $\mu = 1$, $r_{\text{in}} = 0.5$, $\mu_B = 2$, $m = 1$, $Ha = 50$ (always). Perfect-conducting boundary conditions.

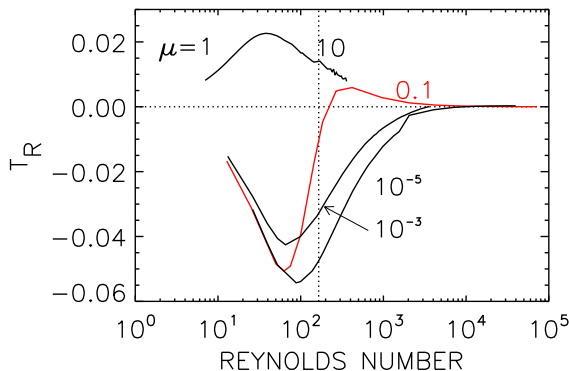


FIGURE 4. Normalized angular momentum transport T_R (averages in the entire container) for the rigidly rotating z -pinch along the line of neutral instability $Re = Re_{\max}$. The curves are marked with Pm . The radial momentum flux vanishes close to the magnetic sonic point (the vertical dotted line) for $Pm = 0.1$. The T_R curves are invariant against the transformation $m \rightarrow -m$. $\mu = 1$, $\mu_B = 2$, $r_{\text{in}} = 0.5$, $m = \pm 1$. Perfect-conducting boundary conditions.

momentum transport T_R should vanish for all values of the parameters if the z -pinch rotates with uniform Ω but this is not confirmed by the calculations.

3.2. Λ effect for rigid-body rotation

The left panel of Fig. 3 gives the normalized radial fluxes of angular momentum between the two cylinders for the rigidly rotating z -pinch for various magnetic Prandtl numbers and for one and the same (small) Hartmann number, $Ha = 50^\dagger$. It is positive for large Pm , it is negative for $Pm \lesssim 0.1$ and it almost vanishes for very small Pm . As we know, for very small Pm the angular momentum transport is dominated by the Reynolds stress, while for large Pm the magnetic terms exceed the kinetic ones. Then only the negativity of the Reynolds stress produces negative T_R . For large magnetic Prandtl numbers it can be overcompensated by negative Maxwell stress

\dagger the maximal Reynolds number for $Pm = 0.1$ is $Re_{\max} = 144$

$\langle b_R b_\phi \rangle$. Note, that there is no shear which could explain the anticorrelation of the fluctuations b_R and b_ϕ .

The right panel of Fig. 3 demonstrates that the calculations along the line of neutral stability ($\text{Re} = \text{Re}_{\text{max}}$) may underestimate the numerical values of the possible (normalized) angular momentum fluxes. The $T_R(R)$ is computed along a vertical cut for $\text{Ha} = 50$ and $\text{Pm} = 0.1$. The curves are marked with the used values of the Reynolds number. The two red lines in both panels of Fig.3 are identical. Of course, $T_R = 0$ for $\text{Re} = 0$. The remaining curves for $\text{Re} = 50$ and $\text{Re} = 100$ yield larger numerical values as the curve for the neutral line, for $\text{Re} = \text{Re}_{\text{max}}$. The growth rates of the instability pattern for these curves do not vanish.

Figure 4 presents the normalized angular momentum transport T_R for rigid rotation along the lines of neutral stability for several values of the magnetic Prandtl number. The T_R is now averaged over the entire container. The vertical dotted line gives for $\text{Pm} = 0.1$ the magnetic sonic point where $\text{Mm} = 1$. For the same Pm the red line shows positive values for large magnetic Mach numbers and negative values for small magnetic Mach numbers. The figure also provides nonvanishing T_R for $\text{Pm} \neq 0.1$. For $\text{Pm} < 0.1$ even for faster rotation the T_R remains negative. For $\text{Pm} = 10$ the T_R is also finite but it is positive. The reason is that the magnetic sonic point for $\text{Pm} = 10$ occurs already for $\text{Re} = 13$ hence the main part of the corresponding curve belongs to super-Alfvénic flows. For $\text{Pm} = 10^{-6}$ the magnetic sonic point is located at $\text{Re} \simeq 20.000$.

For a more detailed discussion Fig. 5 gives the ratio

$$\varepsilon_{\text{AMT}} = \frac{\langle b_R b_\phi \rangle}{\mu_0 \rho \langle u_R u_\phi \rangle} \quad (3.1)$$

of the Maxwell stress and the Reynolds stress versus the Reynolds number for the containers with $\text{Pm} = 0.1$ and $\text{Pm} = 10$. Striking differences only exist in the vicinity of the magnetic sonic point with $\text{Mm} = 1$ (vertical dotted lines in Figs. 4 and 5). For larger as well as for smaller Reynolds numbers it is $0 < \varepsilon_{\text{AMT}} < 1$, hence the Reynolds stress (slightly) exceeds the Maxwell stress. For the (normalized) stresses it is

$$\langle u_R u_\phi \rangle \propto \frac{T_R}{1 - \varepsilon_{\text{AMT}}}, \quad \frac{\langle b_R b_\phi \rangle}{\mu_0 \rho} \propto \varepsilon_{\text{AMT}} \frac{T_R}{1 - \varepsilon_{\text{AMT}}}. \quad (3.2)$$

For small $\varepsilon_{\text{AMT}} > 0$ it is $\langle u_R u_\phi \rangle \propto T_R$ and also $\langle b_R b_\phi \rangle \propto T_R$. Both stresses possess the same sign. This case is realized along almost the whole red line of Fig. 5. Left from the vertical dotted line both stresses are negative and right from the dotted line both stresses are positive. A negative Maxwell stress for all sub-rotation laws is easy to understand by the induction process due to differential rotation but it even exists for slow and rigid rotation. On the other hand, for large $|\varepsilon_{\text{AMT}}|$ the Maxwell stress dominates and it is simply $\langle b_R b_\phi \rangle \simeq -T_R$ so that $\langle b_R b_\phi \rangle > 0$ for $T_R < 0$ (left from the dotted line) and $\langle b_R b_\phi \rangle < 0$ for $T_R > 0$. The sign of the Maxwell stress changes where the red line crosses the horizontal solid line for $\varepsilon_{\text{AMT}} = 0$. This is

The zeros of T_R in the Fig. 4 (horizontal dotted line) are defined by $\varepsilon_{\text{AMT}} = 1$ which happens close to the sonic point $\text{Mm} = 1$. For larger Mm the Reynolds stress exceeds the Maxwell stress and it is positive leading to $T_R > 0$. For $\text{Mm} \simeq 1$ the magnetic stress becomes important and it is $\langle b_R b_\phi \rangle > 0$ leading to negative T_R . For even smaller Mach numbers again the Reynolds stress exceeds the Maxwell stress but both are now negative.

Large values $\varepsilon_{\text{AMT}} > 1$ for $\text{Pm} = 10$ shown in Fig. 5 indicate the dominance of the Maxwell stress for the angular momentum transport. The positive T_R values for large Pm result from a large anticorrelation of the magnetic perturbations b_R and b_ϕ despite of the rigid rotation.

All these findings are rather general as free parameters do not enter the calculations of the ratio ε_{AMT} . The question arises whether the diffusion approximation (1.4) must be modified by an additional term

$$T_{ij} = \dots + A_{ijk} \Omega_k, \quad (3.3)$$

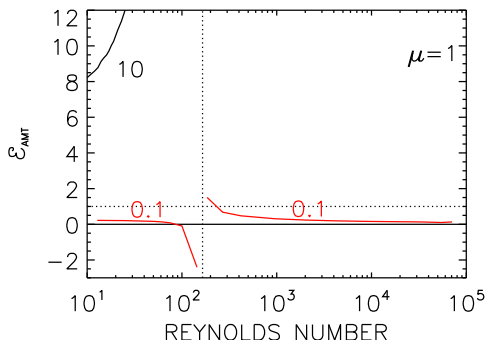


FIGURE 5. Stress ratios (3.1) along the lines of neutral stability for $\text{Pm} = 0.1$ and $\text{Pm} = 10$ with averages over the container. The horizontal dotted line gives $\varepsilon_{\text{AMT}} = 1$, the vertical line denotes the magnetic sonic point ($\text{Re} = 180$) for $\text{Pm} = 0.1$. $r_{\text{in}} = 0.5$, $\mu = 1$, $\mu_B = 2$, $m = 1$. Perfect-conducting boundary conditions.

in the stress tensor T_{ij} which does not vanish for rigid rotation (“ Λ effect”). We have seen that indeed for the rigidly rotating z -pinch such a Λ effect exists with a strong dependence on the magnetic Prandtl number.

The Λ effect is known to appear in rotating convective spheres which are basically anisotropic in the radial direction \mathbf{g} due to the density stratification. The tensor $A_{ijk} = (\epsilon_{ikl}g_j + \epsilon_{jlk}g_i)g_l$ appears in the stress tensor leading to cross correlations $T_{r\phi}$ also at the equator. For unstratified but magnetized turbulences a very similar tensor may exist after the transformation $\mathbf{g} \rightarrow \mathbf{B}$, i.e. $A_{ijk} = (\epsilon_{ikl}B_j + \epsilon_{jlk}B_i)B_l$. The radial flux of angular momentum for toroidal fields is thus $T_{R\phi} \propto B_\phi^2\Omega$ suggesting that the results obtained from Fig. 3 perform a new magnetic-induced realization of the Λ effect.

The amplitudes of the normalized T_R in Fig. 3 for rigid rotation are smaller by one order of magnitude than those for quasi-Keplerian rotation (see below) but they are not very small. About 2% of the kinetic and magnetic energy are included in the cross correlation of radial and azimuthal components which, also in comparison with rotating convection, does not seem as unreasonable. Depending on the rotation rate Käpylä (2019) obtains cross correlations $Q_{r\phi}$ of 1...10 % of the turbulence energy. The sign of the perturbation-induced radial fluxes T_R , however, strongly depends on the value of Pm while for rotating convection it is negative-semidefinite as numerical simulations show (Chan 2001; Hupfer *et al.* 2006). At the equator and for fast rotation, however, the $T_{r\phi}$ generated by convection almost vanishes.

4. Nonuniform rotation

Among the possible rotation laws the quasi-Keplerian rotation is of particular interest in astrophysics. In a Taylor-Couette setup this flow is approximated by the assumption that the two cylinders rotate around the central axis like planets, hence $\mu = r_{\text{in}}^{1.5}$. For $r_{\text{in}} = 0.5$ the rotation ratio for such quasi-Keplerian flows is $\mu = 0.35$. This rotation may be influenced by two different magnetic field profiles. The first example is given by the z -pinch with $\mu_B = 2$ while the second model may fulfill the condition (2.8), i.e. $\mu_B = 0.7$ for $r_{\text{in}} = 0.5$. Only the latter model belongs to the class of Chandrasekhar-type flows.

The stability map for the field profiles fulfilling the Chandrasekhar condition combines typical properties of the maps for AMRI and Tayler instability. The left top panel of Fig. 6 gives the lines of neutral stability for the field with $\mu_B = 0.7$. The curves for all Pm possess crossing points

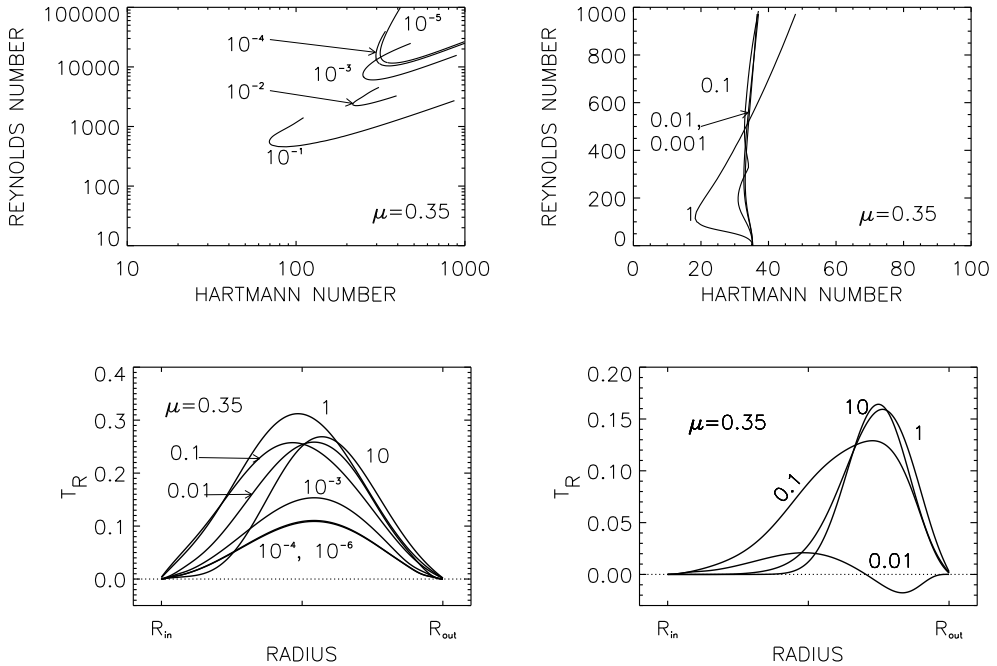


FIGURE 6. Top: Stability maps for the quasi-Keplerian rotation with $\mu_B = 0.7$ (left, Chandrasekhar-type) and $\mu_B = 2$ (z -pinch, right). For the pinch it is $Ha_0 = 35.3$. The curves are marked with their values of Pm. Bottom: Radial angular momentum transport by quasi-Keplerian rotation for $\mu_B = 0.7$ (left) and $\mu_B = 2$ (right). The Hartmann numbers are $Ha = Ha_{min}$ for $\mu_B = 0.7$ and $Ha = 50$ for $\mu_B = 2$. $r_{in} = 0.5$, $\mu = 0.35$, $m = \pm 1$. Perfect-conducting cylinders.

Ha_0 with the horizontal axis ($Re = 0$, not visible) but they also possess the absolute minimum Hartmann numbers Ha_{min} with $Ha_{min} < Ha_0$. The curves for very small Pm coincide. For small magnetic Prandtl numbers the Ha_{min} (and also the associated Reynolds numbers) for the Chandrasekhar flow are rather small. Chandrasekhar-type fields are thus more unstable than fields which are current-free between the cylinders (Kirillov & Stefani 2013). Even more unstable is the z -pinch with $\mu_B = 2$ combined with quasi-Keplerian rotation where the instability is excited for very small Hartmann numbers $Ha_0 = 35.3$ (independent of the magnetic Prandtl number, top right panel of Fig. 6).

The first question is whether the quasi-Keplerian flow with $\mu_B = 0.7$ also provides an anomalous angular momentum transport as the rigidly rotating z -pinch which is also of the Chandrasekhar-type. For many Pm the angular momentum transport has thus been calculated at $Ha = Ha_{min}$ (Fig. 6, bottom panel left) and for $Ha = 50$ (Fig. 6, bottom panel right). The results provide positive T_R for all Pm without any exception. An anomalous angular momentum transport does thus not exist for the two given examples with quasi-Kepler rotation law.

In order to demonstrate the basic influence of the magnetic Prandtl number on the contribution of the Maxwell stress to the angular momentum transport Fig. 7 gives the stress ratio ε_{AMT} for the Chandrasekhar-type flow with quasi-Keplerian rotation and the z -pinch. Up to a magnetic Prandtl number of 10^{-2} the Maxwell stress is not important but for larger Pm it is (because of $|\varepsilon_{AMT}| \gg 1$). Yet for these examples with growing magnetic Prandtl number also the magnetic Reynolds number grows. Moreover, one always finds $\varepsilon_{AMT} < 0$ so that $\langle u_R u_\phi \rangle > 0$ and $\langle b_R b_\phi \rangle < 0$ for all magnetic Prandtl numbers. Both the Reynolds stress as well as the Maxwell stress are

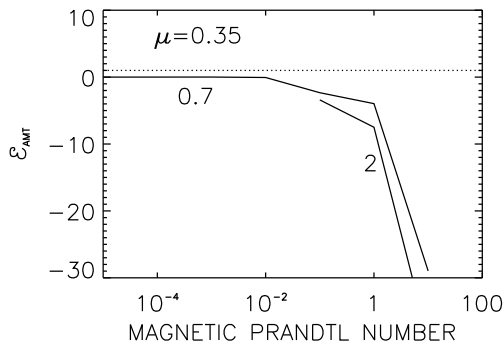


FIGURE 7. Container-averaged stress ratios (3.1) for the quasi-Keplerian flows characterized in Fig. 6. The Hartmann numbers are $\text{Ha} = \text{Ha}_{\min}$ for the Chandrasekhar-type flows ($\mu_B = 0.7$) and $\text{Ha} = 50$ for the z -pinch ($\mu_B = 2$). The horizontal dotted line symbolizes the ratio being unity, $\varepsilon_{\text{AMT}} = 1$. $\mu = 0.35$, $m = \pm 1$, $r_{\text{in}} = 0.5$. Insulating cylinders.

thus transporting angular momentum outwards. As expected for negative shear, b_R and b_ϕ are anticorrelated. Mainly the Maxwell stress transports the angular momentum outward but this is only true for large magnetic Prandtl numbers.

After the Boussinesq relation (1.4) a z -pinch with negative shear generates positive T_R for all Pm. At least for $\text{Pm} = 0.1$ there must thus a transition exist between the negative values for rigid rotation and the positive values for, e.g., Kepler rotation as shown by the right panel of Fig. ???. The questions arise if this transition is monotonous and for which rotation law the angular momentum flux vanishes. For the rotation laws with $\mu = 1, \mu = 0.9, \dots, 0.35$ the normalized values of T_R are given in Fig. 8 within the cylindrical gap for $\text{Ha} = 50$.

One finds T_R vanishing for $\mu \simeq 0.75$. If (1.4) is modified to

$$T_R = \Lambda \Omega - \nu_T R \frac{d\Omega}{dR}, \quad (4.1)$$

then $\nu_T = \Lambda \, d \log R / d \log \Omega$ for $\mu = 0.75$. In the sense of an heuristic estimate $d \log \Omega / d \log R \simeq -2/3$ is used so that

$$\nu_T \simeq 0.05 \frac{E}{\Omega} \quad (4.2)$$

follows with the total turbulence energy E (see Sect. 3). If E can be replaced by P/ρ with P as the turbulence pressure then Eq. (4.2) can be read as a confirmation of the viscosity approximation introduced by Shakura & Sunyaev (1973). Note that the numerical coefficient in Eq. (4.2) is basically smaller than unity. Though with a linear theory the function $E = E(\Omega)$ cannot be determined so that the numerical calculation of the eddy viscosity must remain open. If it should be allowed to work with the phase velocity ω_{dr}/k (the ratio of the drift frequency and the wave number) for the r.m.s. velocity then

$$\frac{\nu_T}{\nu} \simeq 0.05 \left(\frac{\omega_{\text{dr}}}{k} \right)^2 \text{Re} \quad (4.3)$$

with ω_{dr}/k in code units. The latter ratio proved to be rather smooth along the neutral line, with a characteristic value of 0.02 for $\text{Re} = \mathcal{O}(10^4)$. Hence, $\nu_T/\nu \simeq 10^{-3} \text{Re}$, in rough agreement to nonlinear results (Rüdiger *et al.* 2018).

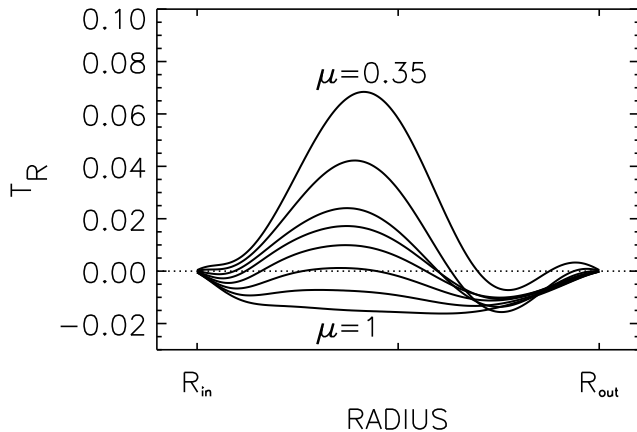


FIGURE 8. The normalized angular momentum transport for nonuniformly rotating z -pinches with $\mu = 1$ to $\mu = 0.35$ (marked). $\mu_B = 2$, $\text{Ha} = 50$, $m = \pm 1$, $\text{Pm} = 0.1$, $r_{\text{in}} = 0.5$. Perfect-conducting cylinders.

5. Conclusions

We have shown that for the magnetic instability of azimuthal fields the angular momentum transport can often be modeled by the diffusion approximation (1.4) but not always. Exceptions exist for rigidly rotating tubes with radially increasing magnetic toroidal magnetic fields where the axial background current flows in the fluid parallel to the rotation axis. The resulting nonvanishing radial angular momentum flux excludes the uniform rotation as a solution of the MHD equation system of the rotating pinch.

For reasons of consistency our models are mostly located at the lines of neutral stability for given radial profiles of U_ϕ and B_ϕ where the growth rates vanish. In one case we also proceeded along a vertical cut in the (Ha/Re) plane with a fixed Hartmann number ($\text{Ha} = 50$) for Reynolds numbers smaller than Re_{max} where the growth rates are positive. The results demonstrate the existence of normalized angular momentum fluxes even exceeding the values $T_R(\text{Re}_{\text{max}})$.

Among the fields which we probe for angular momentum transport are also those of the Chandrasekhar-type where the magnetic field B_ϕ has the same radial profile as the linear velocity U_ϕ of the rotation. The instability curves of such Chandrasekhar-type systems coincide for small Pm in the (Ha/Re) plane. Prominent examples of this particular class of MHD flows are the rigidly rotating z -pinch (flow and field are linearly running with R) and also the quasi-Keplerian rotation combined with a magnetic field running with $1/\sqrt{R}$. For both constellations one finds finite values of the angular momentum transport. It is positive (outward flow of angular momentum) for the quasi-Keplerian rotation for all Pm and for the uniformly rotating pinch but only for large magnetic Mach number. For slow rigid rotation and not too large Pm it is negative, i.e. the angular momentum flows inward.

For small magnetic Prandtl number the contribution of the Maxwell stress to the angular momentum flow is only small but the Reynolds stress $\langle u_R u_\phi \rangle$ is negative. For the larger Pm the transport is always outward due to the dominating negative Maxwell stress, $\langle b_R b_\phi \rangle < 0$, as expected for rotation with negative shear.

We have checked the surprising finding for rigid rotation also with the the quasi-uniform field as another prominent magnetic field profile ($\mu_B = \mu = 1$). Flow and field of this model (which is not of the Chandrasekhar-type) are only unstable for $\text{Mm} < 0.5$. Again a finite angular momentum transport exists which again is directed inward for $\text{Pm} = 0.1$ (Fig. 9). Obviously,

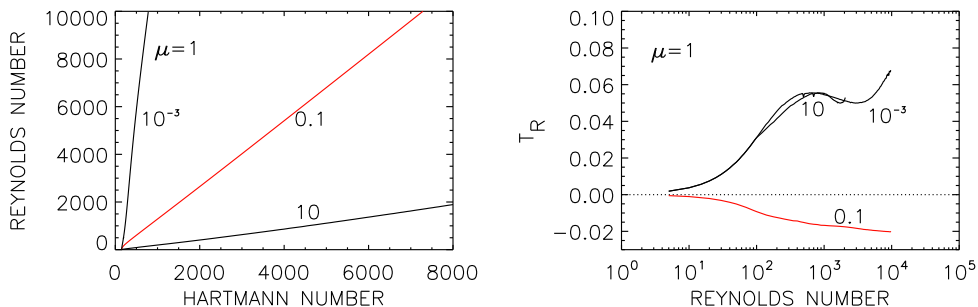


FIGURE 9. Stability map (left) and radial angular momentum transport (right) for uniform rotation and quasi-uniform magnetic field for various magnetic Prandtl numbers. Flows with Reynolds numbers above the lines are stable. It is $Ha_0 = 150$ for $Re = 0$. The curves are marked with their values of Pm . $\mu = \mu_B = 1$, $m = \pm 1$, $r_{in} = 0.5$. Perfect-conducting cylinders.

the radial profile of the magnetic field does not play the decisive role for the existence of the Λ effect of magnetic instability.

The phenomenon that a *rigidly* rotating z -pinch for a given magnetic Mach number transports angular momentum cannot be described by the diffusion approximation (1.4). It forms a magnetic counterpart to the hydrodynamical Λ effect in rotating anisotropic turbulences. It means that solid-body rotation can neither be maintained in rotating convection zones nor in rotating tanks with a conducting fluid and a supercritical electric current flowing in z -direction.

It makes also sense to study the transition of the angular momentum flux from uniform rotation (inward transport) to quasi-Keplerian rotation (outward transport). Figure 8 demonstrates how the anomalous angular momentum transport disappears if the rotation law becomes more and more nonuniform. At a certain shear value the angular momentum flux vanishes. For the z -pinch with $Pm = 0.1$ the transport vanishes for $\mu \simeq 0.75$ where Λ effect and viscous transport compensate each other. This result can be used for an approximated evaluation of the eddy viscosity. The related expression formally explains the formulation of Shakura & Sunyaev (1973) and numerical values (by use of the phase velocity as the r.m.s. velocity of the instability) only slightly differ from the results of nonlinear simulations presented earlier.

REFERENCES

- BOUSSINESQ, M. 1897 *Theorie de lecoulement tourbillonnant et tumultueux des liquides dans les lits rectilignes a grande section*. Gauthier-Villars, Paris.
- CHAN, K. L. 2001 Rotating Convection in F-Planes: Mean Flow and Reynolds Stress. *The Astrophysical Journal* **548**, 1102–1117.
- CHANDRASEKHAR, S. 1956 On the Stability of the Simplest Solution of the Equations of Hydromagnetics. *Proc. Natl. Acad. Sci. USA* **42**, 273–276.
- CHARBONNEAU, P. & MACGREGOR, K. B. 1992 Angular momentum transport in magnetized stellar radiative zones. I - Numerical solutions to the core spin-up model problem. *The Astrophysical Journal* **387**, 639–661.
- DEGUCHI, K. 2017 Linear instability in Rayleigh-stable Taylor-Couette flow. *Physical Review E* **95** (2), 021102.
- HERRON, I. & SOLIMAN, F. 2006 The stability of couette flow in a toroidal magnetic field. *Appl. Math. Lett.* **19**, 1113–1117.
- HUPFER, C., KÄPYLÄ, P. J. & STIX, M. 2006 Reynolds stresses and meridional circulation from rotating cylinder simulations. *Astronomy & Astrophysics* **459**, 935–944.
- Ji, H., GOODMAN, J. & KAGEYAMA, A. 2001 Magnetorotational instability in a rotating liquid metal annulus. *Month. Not. Roy. Astr. Soc.* **325**, L1–L5.

- KÄPYLÄ, P. J. 2019 Magnetic and rotational quenching of the Λ effect. *Astronomy & Astrophysics* **622**, A195, arXiv: 1712.08045.
- KIRILLOV, O. N. & STEFANI, F. 2013 Extending the Range of the Inductionless Magnetorotational Instability. *Physical Review Letters* **111** (6), 061103, arXiv: 1303.4642.
- OGILVIE, G. I. & PRINGLE, J. E. 1996 The non-axisymmetric instability of a cylindrical shear flow containing an azimuthal magnetic field. *Month. Not. Roy. Astr. Soc.* **279**, 152–164.
- PITTS, E. & TAYLER, R. J. 1985 The adiabatic stability of stars containing magnetic fields. IV - The influence of rotation. *Month. Not. Roy. Astr. Soc.* **216**, 139–154.
- PRINGLE, J. E. 1981 Accretion discs in astrophysics. *Ann. Rev. Astronomy Astrophysics* **19**, 137–162.
- RÜDIGER, G., GELLERT, M., HOLLERBACH, R., SCHULTZ, M. & STEFANI, F. 2018 Stability and instability of hydromagnetic Taylor-Couette flows. *Physics reports* **741**, 1–89, arXiv: 1703.09919.
- RÜDIGER, G., HOLLERBACH, R., SCHULTZ, M. & ELSTNER, D. 2007 Destabilization of hydrodynamically stable rotation laws by azimuthal magnetic fields. *Month. Not. Roy. Astr. Soc.* **377**, 1481–1487.
- RÜDIGER, G. & KITCHATINOV, L. L. 1996 The Internal Solar Rotation in Its Spin-down History. *The Astrophysical Journal* **466**, 1078.
- RÜDIGER, G. & SHALYBKOV, D. A. 2001 MHD Instability in cylindrical Taylor-Couette flow. *12th International Couette-Taylor Workshop, Evanston 2001 –*, arXiv: astro-ph/0108035.
- RÜDIGER, G. & ZHANG, Y. 2001 MHD instability in differentially-rotating cylindrical flows. *Astronomy & Astrophysics* **378**, 302–308.
- SEILMAYER, M., GALINDO, V., GERBETH, G., GUNDRUM, T., STEFANI, F., GELLERT, M., RÜDIGER, G., SCHULTZ, M. & HOLLERBACH, R. 2014 Experimental Evidence for Nonaxisymmetric Magnetorotational Instability in a Rotating Liquid Metal Exposed to an Azimuthal Magnetic Field. *Physical Review Letters* **113** (2), 024505.
- SEILMAYER, M., STEFANI, F., GUNDRUM, T., WEIER, T., GERBETH, G., GELLERT, M. & RÜDIGER, G. 2012 Experimental Evidence for a Transient Tayler Instability in a Cylindrical Liquid-Metal Column. *Physical Review Letters* **108** (24), 244501.
- SHAKURA, N. I. & SUNYAEV, R. A. 1973 Black holes in binary systems. Observational appearance. *Astronomy & Astrophysics* **24**, 337–355.
- STEFANI, F. & KIRILLOV, O. N. 2015 Destabilization of rotating flows with positive shear by azimuthal magnetic fields. *Physical Review E* **92** (5), 051001.
- TAYLER, R. J. 1957 Hydromagnetic Instabilities of an Ideally Conducting Fluid. *Proceedings of the Physical Society B* **70**, 31–48.
- TAYLER, R. J. 1973 The adiabatic stability of stars containing magnetic fields-I.Toroidal fields. *Month. Not. Roy. Astr. Soc.* **161**, 365.
- VELIKHOV, E. 1959 Stability of an ideally conducting liquid flowing between cylinders rotating in a magnetic field. *Soviet. Phys. JETP* **36**, 1389–1404.

$Pm=0.1, \mu_{\Omega}=1, \eta=0.5, \mu_B=1, \text{cond}$

